Three-Dimensional Images for Electron-Impact Single Ionization of He: Complete and Comprehensive $(e, 2e)$ Benchmark Data

M. Dürr, C. Dimopoulou, B. Najjari, A. Dorn, and J. Ullrich
Max-Planck-Institute for Nuclear Physics, Saupfercheckweg 1, 69117 Heidelberg, Germany
(Received 16 November 2005; published 21 June 2006)

Comprehensive fully differential cross sections for electron emission into all three spatial dimensions are presented for 1 keV and 102 eV electron-impact single ionization of helium using an advanced reaction microscope. Surprising out-of-plane contributions, traced back to an interference term in a perturbation expansion by comparison with ion-impact data, severely challenge theoretical models that accurately predict coplanar emission. The data represent the ultimate benchmark for recently developed exact theoretical descriptions of the most fundamental three-body quantum problems.

DOI: 10.1103/PhysRevLett.96.243202 PACS numbers: 34.80.Dp, 34.80.Pa

It was not until 1999 [1] and 2002 [2] that the basic dynamic three-body problem in quantum mechanics was claimed to be exactly solved numerically [1] and formally understood [2] as it is realized, e.g., in electron-impact single ionization of atomic hydrogen or photodouble ionization of helium, respectively. Theoretically, tremendous progress has been achieved within the last decade in describing singly ionizing collisions, going far beyond early first-order Born approximation (FBA) results. Among the most sophisticated approximate theories are the so-called three Coulomb wave function (3C) methods [3], which include to all orders the pairwise Coulomb interactions between the scattered projectile, the leftover ion and the ionized slow electron in the final state, R matrix as well as distorted wave techniques (e.g., [4,5]). Progress culminated into the development of ''exact'' formalisms, namely, the exterior complex scaling (ECS) [1] and convergent-close coupling (CCC) [2] coupled channel approaches. Predictions of both are in excellent agreement with all available experimental data [6]. However, such large-scale computer calculations, based on partial wave expansion techniques, have not been yet applicable for high-energy electron or heavy-particle impact.

Experimentally, the field has been stimulated by the development of many-particle imaging techniques, so-called ''reaction microscopes'' (for a recent review, see [7]). Projecting all charged fragments of any atomic or molecular reaction by electric and magnetic fields onto position and time-sensitive detectors, their complete vector momenta can be recorded simultaneously with high resolution for a large part of the many-particle final state momentum space. Thus, electron emission can be imaged in all three spatial dimensions (3D) and fully differential cross sections (FDCS) are obtained for any geometrical situation. Moreover, it became possible to record FDCS for heavy-particle impact by deducing, via momentum conservation, the inaccessibly small projectile scattering angle from the momenta of the recoiling target ion and the slowly emitted target electron.

It then came as a big surprise that 3D images of low-energy electron emission in single ionization of He by ion impact (100 MeV/u C^{6+}) revealed distinct features out of the scattering plane which is spanned by the incoming and scattered projectile momentum vectors $\vec{p}_0$ and $\vec{p}_1$, respectively (Fig. 2) [8]. In principle, at a projectile velocity of $v_P = 60$ a.u. and a projectile charge of $Z_P = 6$ one is in a ''simple'' situation, where the perturbation parameter Z_P/v_P is small and even the FBA should hold (expected to be valid for $Z_P/v_P \ll 1$; atomic units are used throughout: $m_e = q_e = \hbar = 1$ with m_e and q_e the electron mass and charge, respectively, and $\hbar$ Planck's constant). Nonetheless, not only did the FBA fail, but, more troubling, all the above mentioned sophisticated approximate calculations going well beyond a first-order treatment and expected to be perfectly suited to describe FDCS at high energies were found to be in striking disagreement with the experimental results, initiating a lively debate and considerable efforts. While it is clear from symmetry reasons that the contributions of higher order in a Born expansion series must be responsible for the strong emission perpendicular to the scattering plane and such contributions are known to be important for He double ionization at similar projectile energies, so far no quantitative theoretical description has emerged [9–11]. Moreover, exact theoretical results are not available for the two reasons mentioned above, namely, high impact energy and heavy projectiles. On the other hand, electron-impact data in out-of-plane geometry are scarce using conventional methods [12] and have not been accessible either with standard reaction microscopes at low projectile energies.

In this Letter, we present comprehensive, absolutely normalized 3D images for electron-impact single ionization of He at different energies, providing complete, ultimate benchmark data for exact theories on the simplest quantum dynamical three-particle problem in a four-body system. At 1 keV impact energy we tackle the troubling situation of ion-impact single ionization since our data can now be directly compared with these puzzling results and

the theoretical approximation methods used to explain them. Observing similar but quantitatively weaker out-of-plane structures compared to ion impact, we then extend the study to lower impact energies, at 102 eV. Here, higher-order effects in a Born expansion series become more important making ''approximate'' theories typically less reliable, but exact theories should be applicable and the responsible dynamical mechanisms might be revealed more easily.

The experiment was performed using a multicoincidence multielectron recoil-ion momentum spectrometer also known as reaction microscope (Fig. 1) [7]. A well-focused (1 mm), pulsed electron beam (pulse length ≈ 1.5 ns, repetition rate $= 200$ kHz, $\approx 10^4$ electrons/pulse), produced by a standard thermocathode gun, crosses and ionizes a supersonic He jet (1 mm diameter, 10^{12} atoms/cm^3). Using parallel electric (1 V/cm) and magnetic (6 G) fields, the fragments in the final state are projected onto 2D position and time-sensitive multihit channel plate detectors equipped with a delay-line readout. In this way, a large part of the full solid angle is covered, 100% for the detection of target ions and 80% for electrons below 15 eV. From the hitting positions and the time-of-flight the vector momenta of the particles can be calculated.

Different from all previous designs, the present reaction microscope has been decisively improved by guiding the electron projectile beam (defining the longitudinal direction), exactly parallel to the electric and magnetic extraction fields, requiring a central bore (5 mm diameter) in the forward electron detector to allow for the passage of the nondeflected electrons. Thus, any beam energy can be realized, with the present gun between 30 eV and 2 keV, aiming to reach eV beam energies with meV energy resolution from a photocathode in the near future. Moreover, scattered projectile electrons with a transverse momentum of 0.2 a.u. $\leq p_\perp \leq 1.2$ a.u. are detected as well. Therefore, the scattering angle and the momentum transfer can be directly obtained with a resolution that is a factor of 2 to 3 better than the one achievable by reconstruction from the recoil ion and the ejected electron momenta, as it is usually done for ion-impact measurements. For the present experiments as for typical ion-impact data the recoil-ion momentum resolution (FWHM) is $(\Delta p_\perp, \Delta p_\parallel) \approx (0.25, 0.15)$ a.u. For all electrons, including the scattered ones, the transversal resolution is $\Delta p_\perp \approx 0.1$ a.u. The longitudinal resolution for the slow ionized electrons is $\Delta p_\parallel \approx 0.02$ a.u., while for the scattered projectiles at $E_0 = 102$ eV we estimated $\Delta p_\parallel \approx 0.08$ a.u. The unresolved longitudinal momentum for fast scattered projectiles at $E_0 = 1$ keV is no major restriction since, for the small scattering angles considered here, $p_\parallel$ can be obtained from the energy loss of the projectile by $p_\parallel = p_0 - (E_I + E_2)/v_p$ (p_0, incoming projectile momentum; E_I, ionization potential; E_2 ejected electron energy) with $\Delta p_\parallel \leq 0.04$ a.u.

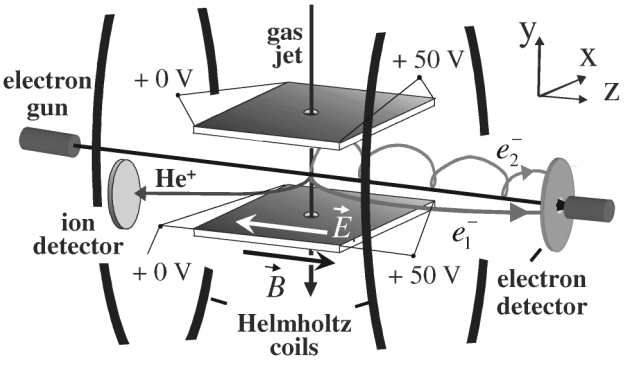

FIG. 1. Schematic view of the experimental setup.

The absolute normalization at 1 keV has been performed with an estimated maximum uncertainty of 15% [13,14], by a controlled extrapolation of the generalized oscillator strength to zero momentum transfer and calibrating the result to accurately known photoionization cross sections [15]. This method becomes unreliable at the $E_0 = 102$ eV, where the collision kinematics is far off the optical limit even for vanishing scattering angle. For this projectile energy the data are normalized to the absolute cross sections measured in coplanar geometry by Röder *et al.* as reported in [16] with a quoted error of 30%.

In Fig. 2, the measured 3D image of the experimental FDCS for He^+ production by 1 keV electrons ($v_P = 8.6$ a.u.) is compared with the corresponding result for 100 MeV/amu C^{6+} impact ($v_P = 60$ a.u.) at about the same perturbation $|Z_P/v_P| \approx 0.1$. In a perturbative treatment, the differential cross section is given by $d\sigma = \alpha_1(Z_P/v_P)^2 + \alpha_2(Z_P/v_P)^3 + \alpha_3(Z_P/v_P)^4 + \cdots$, where the coefficients α are independent of Z_P. If the first Born approximation is valid ($Z_P/v_P \ll 1$), only the leading term of the expansion needs to be considered, and then electron and ion impact should yield identical results for identical kinematical parameters. Thus, for both cross sections presented, the absolute value of the momentum transfer, $|\vec{q}| = |\vec{p}_1 - \vec{p}_0|$, has been fixed to $|\vec{q}| = 0.75$ a.u. and the energy of the emitted electron is $E_2 = 6.5$ eV. Integration intervals of the present electron-impact data are $\Delta|\vec{q}| = \pm 0.2$ a.u. and $\Delta E_2 = \pm 1$ eV. For electron impact due to the lower v_P the momentum transfer $\vec{q}$ is kinematically shifted forward by 12° with respect to $\vec{q}$ in the ion collision which is almost perpendicular to the incoming beam. In order to simplify the comparison we have removed this difference in all figures by rotating the electron-impact cross section correspondingly.

Both emission patterns are governed by the well-known double-lobe structure which can be quantitatively reproduced within a first-order description: the large lobe (the so-called binary lobe) in the direction of $\vec{q}$ corresponds to electrons emitted in a single binary collision with the projectile; i.e., the target nucleus essentially remains a spectator. If the ionized electron additionally backscatters in the ionic potential, this gives rise to the so-called recoil lobe pointing roughly in the direction of $-\vec{q}$. Furthermore,

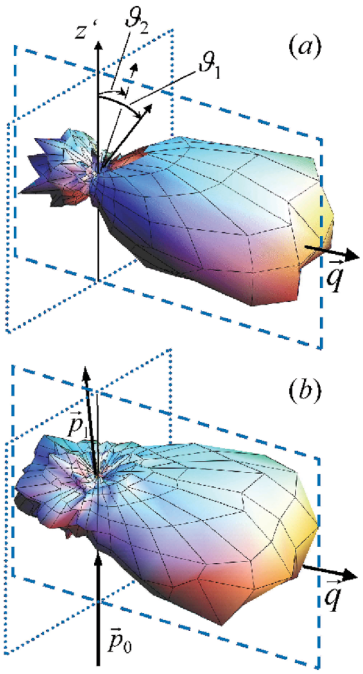

FIG. 2 (color). Comparison of three-dimensional images of electron emission from single ionization of He by 1 keV electrons (a) and 100 MeV/amu C^{6+} ions from [8] (b) on the same absolute scale. The momentum transfer $q = 0.75$ a.u. and the emitted electron energy $E_b = 6.5$ eV are fixed. $\vec{p}_0$, $\vec{p}_1$: incoming and scattered projectile momentum. The scattering plane and the plane perpendicular to $\vec{q}$ are indicated by dashed and dotted lines, respectively.

for ion impact, a relatively large intensity perpendicular to the projectile scattering plane was observed for the first time in disagreement with all theoretical predictions up to now. Since this structure violates the axial symmetry with respect to the direction of $\vec{q}$ which is characteristic for first-order processes, this feature is a clear signature of a higher-order process.

For 1 keV electron impact a similar but weaker structure perpendicular to the projectile scattering plane is observed as well [Fig. 2(a)]. For a more quantitative discussion, we present in Fig. 3 cuts of the electron-impact cross section in the scattering plane (dashed lines in Fig. 2) and in the plane perpendicular to $\vec{q}$ (dotted lines in Fig. 2). The cross sections are plotted as a function of the emission angles ϑ_1 (scattering plane) or ϑ_2 (perpendicular plane) with respect to the z' axis which is lying in the scattering plane perpendicular to $\vec{q}$ [see Fig. 2(a)]. The experimental data shown in Fig. 3 are compared to calculations in the FBA (dashed curves) and using the 3C wave function (solid curves) in its standard form [3] with a two parameter ground-state wave function [type (*d*) in [17]]. For all cuts presented, experimental as well as theoretical cross sections have been integrated over an angular range $\pm 10°$ above and below the cutting planes. In the scattering plane [Fig. 3(a)], the agreement of the absolute experimental cross sections with the 3C calculation is good, as expected at these relatively large impact energies (see, e.g., [18]). The observed symmetry with respect to the direction of $\vec{q}$ is a well-accepted indication that the first-order process dominates and higher orders are of minor importance. However, in the plane perpendicular to $\vec{q}$ [Fig. 3(b)] the cross section exhibits distinct maxima close to $\vartheta_2 = 90°$ and 270° with respect to the incoming projectile direction. These maxima clearly indicate the presence of higher-order processes, since they violate the cylindrical symmetry with respect to $\vec{q}$. The 3C calculation fails drastically to reproduce these structures, albeit it predicts some deviation from the isotropic cross section.

The significant difference in the absolute magnitude of the FDCS features in the plane perpendicular to $\vec{q}$ between electron and ion impact must be attributed to the projectile charge-sign dependent $(Z_P/v_P)^3$ term (or any higher odd order) in the perturbation series since the two cases differ in the sign of Z_P/v_P. Accordingly, the contribution in this emission plane originates from the interference between different orders of the projectile-target interaction. Voitkiv *et al.* [9] have demonstrated the charge-sign dependence of the cross section in the plane perpendicular to $\vec{q}$ using perturbative models going beyond the FBA by including projectile-nucleus scattering contributions (Glauber, Eikonal and second Born approximations). While their results qualitatively reproduce the maxima for negative projectile impact, for positive ion impact, however, minima

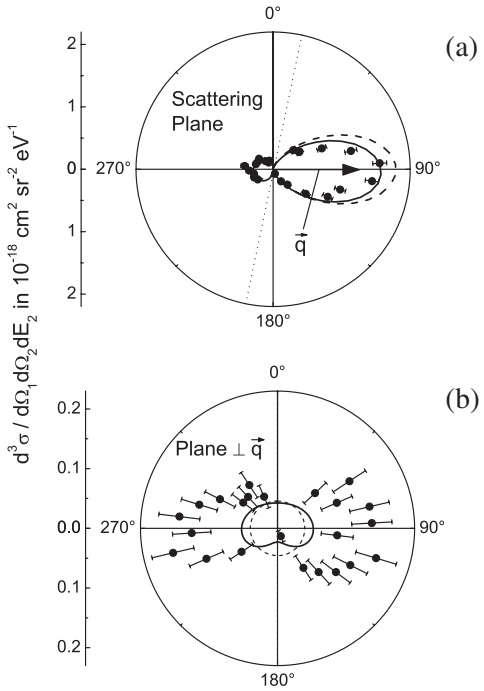

FIG. 3. Selected cuts of the three-dimensional cross section for electron impact in Fig. 2(a). The absolute, fully differential cross section inside the scattering plane (a) and in the plane perpendicular to the momentum transfer $\vec{q}$ (b). Dotted line: incoming projectile direction. Dashed curves: FBA result. Solid curves: 3C result (see text).

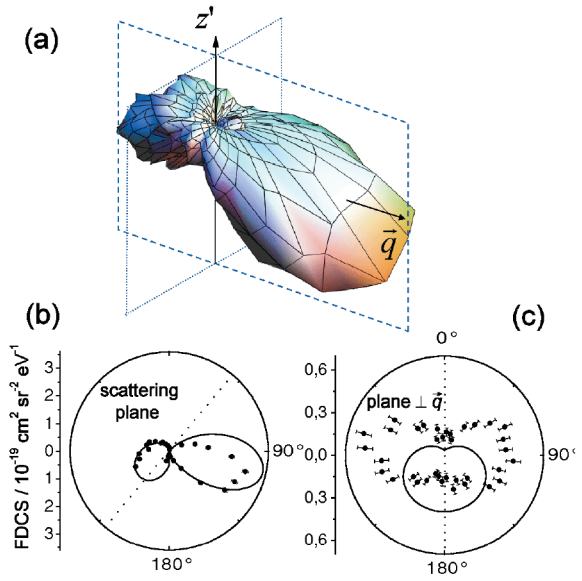

FIG. 4 (color). Electron emission from single ionization of He by 102 eV electron impact. The deflection angle of the scattered projectile is 20° (corresponding to $q = 1.0$ a.u.) and the energy of the emitted electron is $E_2 = 10$ eV. (a) Three-dimensional cross section image. (b) Cut in the scattering plane [dashed line in (a)]. (c) Cut in the plane perpendicular to $\vec{q}$ [dotted line in (a)]. Dotted line in (b) and (c): incoming projectile axis. Solid curves: 3C results (see text).

instead of maxima are predicted in the perpendicular plane at $\vartheta_2 = 90°$ and 270°.

For reduced projectile energy $E_0 = 102$ eV the 3D cross section pattern [see Fig. 4(a)] displays a qualitatively similar out-of-plane emission. A quantitative examination of the cuts inside the scattering plane [Fig. 4(b)] and in the perpendicular plane [Fig. 4(c)] and the respective cuts for $E_0 = 1$ keV (Fig. 3) show that, relative to the binary peak height, the out-of-plane emission is increased by about a factor of 2. Furthermore, for $E_0 = 102$ eV the projectile is sufficiently slow to strongly interact with both the ejected electron and the residual target ion in the final state, which results in a strong asymmetry of the cross section with respect to the momentum transfer axis. In the scattering plane [Fig. 4(b)], the 3C model qualitatively reproduces the shifts of both lobes away from the scattered projectile direction, which can be interpreted as a result of the electron-electron repulsion in the final state. In the cut applied perpendicular to the momentum transfer [Fig. 4(c)], the out-of-plane emission in the 3D representation appears as pronounced maxima at angles of about $\vartheta_2 = 70°$ and 290°, respectively, which are again not reproduced by the 3C calculation.

Thus, it can be concluded that electron- and ion-impact ionization in the perturbative regime reveals essentially identical fully differential cross sections within the scattering plane, obviously strongly dominated by first-order collisions. On the contrary, in the perpendicular geometry first-order contributions are weak and, hence, strong differences between ion and electron-impact data resulting from higher-order contributions can be observed. As discussed in many previous publications for double ionization (e.g., [19,20]) this should be the result of the projectile charge-sign dependent Z_P^3 (or any higher odd order) term occurring as an interference of amplitudes in a perturbation expansion.

In summary, we have presented comprehensive, absolute three-dimensional experimental FDCS for single ionization of He by electron impact at two different energies applying an advanced reaction microscope. While the observed electron-ion-impact differences can be explained by a projectile charge-sign dependent interference between a first-order and a second-order process, the relative importance of the ionic core and the second helium electron as interaction partners is not clear.

Our data on one of the simplest dynamical quantum systems are of utmost importance to benchmark exact theories, i.e., the recently developed CCC or ECS approaches, respectively, at up to keV impact energies under any kinematical and geometrical conditions. In case of agreement, $(e, 2e)$ of one and two electron systems can be considered as completely understood.

We acknowledge support from the EU within the HITRAP project (HPRI-CT-2001-50036). We thank K. Bartschat, I. Bray, D. H. Madison, R. Moshammer, M. Schulz, and A. Voitkiv for fruitful discussions.

[1] T. N. Rescigno *et al.*, Science **286**, 2474 (1999).
[2] I. Bray, Phys. Rev. Lett. **89**, 273201 (2002).
[3] M. Brauner, J. S. Briggs, and H. Klar, J. Phys. B **22**, 2265 (1989).
[4] K. Bartschat *et al.*, Phys. Rev. A **54**, R998 (1996).
[5] Z. Chen *et al.*, J. Phys. B **37**, 981 (2004).
[6] J. Röder *et al.*, Phys. Rev. Lett. **79**, 1666 (1997).
[7] J. Ullrich *et al.*, Rep. Prog. Phys. **66**, 1463 (2003).
[8] M. Schulz *et al.*, Nature (London) **422**, 48 (2003).
[9] A. B. Voitkiv, B. Najjari, and J. Ullrich, J. Phys. B **36**, 2591 (2003).
[10] R. E. Olson and J. Fiol, J. Phys. B **36**, L365 (2003).
[11] D. H. Madison *et al.*, Phys. Rev. Lett. **91**, 253201 (2003).
[12] A. J. Murray and F. H. Read, Phys. Rev. Lett. **69**, 2912 (1992).
[13] A. Lahmam-Bennani, J. Phys. B **21**, 2145 (1988).
[14] A. Lahmam-Bennani *et al.*, J. Phys. B **20**, 2531 (1987).
[15] K. Jung *et al.*, J. Phys. B **18**, 2955 (1985).
[16] I. Bray and D. V. Fursa, Phys. Rev. Lett. **76**, 2674 (1996).
[17] K. Tavard and B. Najjari, Int. J. Quantum Chem. **60**, 657 (1996).
[18] M. Brauner, J. S. Briggs, and J. T. Broad, J. Phys. B **24**, 287 (1991).
[19] J. H. McGuire, Phys. Rev. Lett. **49**, 1153 (1982).
[20] D. Fischer *et al.*, Phys. Rev. Lett. **90**, 243201 (2003).